Inorg. Chem. **2009**, *48*, 872−878

A Bioaccumulative Cyclometalated Platinum(II) Complex with Two-Photon-Induced Emission for Live Cell Imaging

Chi-Kin Koo,[†] Ka-Leung Wong,[†] Cornelia Wing-Yin Man,[‡] Yun-Wah Lam,[†] Leo King-Yan So,[†] Hoi-Lam Tam,[§] Sai-Wah Tsao,[‡] Kok-Wai Cheah,[§] Kai-Chung Lau,[†] Yang-Yi Yang,[||] Jin-Can Chen,[||] and Michael Hon-Wah Lam*[,†]

Department of Chemistry and Biology, City University of Hong Kong, Tat Chee Avenue, Hong Kong SAR, Department of Anatomy, The University of Hong Kong, Sasson Road, Hong Kong SAR, Department of Physics, Hong Kong Baptist University, Kowloon Tong, Hong Kong SAR, and MOE Key Laboratory of Bioinorganic and Synthetic Chemistry, School of Chemistry and Chemical Engineering, Sun Yat-Sen University, People's Republic of China

Received July 6, 2008

The cyclometalated platinum(II) complex [Pt(**L**)Cl], where H**L** is a new cyclometalating ligand 2-phenyl-6-(1*H*-pyrazol-3-yl)pyridine containing C_{phenyl}, $N_{pyridyl}$, and $N_{pyrazolyl}$ donor moieties, was found to possess two-photon-induced luminescent properties. The two-photon-absorption cross section of the complex in *N,N*-dimethylformamide at room temperature was measured to be 20.8 GM. Upon two-photon excitation at 730 nm from a Ti:sapphire laser, bright-green emission was observed. Besides its two-photon-induced luminescent properties, [Pt(**L**)Cl] was able to be rapidly accumulated in live *HeLa* and NIH3T3 cells. The two-photon-induced luminescence of the complex was retained after live cell internalization and can be observed by two-photon confocal microscopy. Its bioaccumulation properties enabled time-lapse imaging of the internalization process of the dye into living cells. Cytotoxicity of [Pt(**L**)Cl] to both tested cell lines was low, according to MTT assays, even at loadings as high as 20 times the dose concentration for imaging for 6 h.

Introduction

Since the pioneering work of Webb and his co-workers on two-photon laser scanning fluorescence microscopy,[1] multiphoton microscopy has rapidly become an invaluable bioimaging tool for the study of various dynamic biochemical processes in cells, thick tissues, and live animals.[2] Advantageous features of multiphoton bioimaging include the reduction of photobleaching and photodamaging of imaging probes and cellular structures, the capability of penetrating thick tissues, and the ability to bring about precise three-dimensional localized photosensitization, photolysis, ablation, and cutting at the subcellular level.[3−6] Thus, considerable research efforts in recent years have been devoted to the development of new multiphoton luminophores, such as organic dyes,[7] molecular lanthanide complexes,[8] up-conversion lanthanide-based nanomaterials,[9] and quantum dots.[10] Lippard and co-workers demonstrated the use of fluorescein-based Zinpyr (ZP)-type sensors for the detection of endogenous Zn^{II} ions in acute hippocampal slices from adult mice by confocal two-photon microscopy (λ_{ex} = 800 nm).[11] With a similar sensing mechanism, Taki et al. reported a benzoxazole-based Zinbo-type sensor, which was capable of in vitro Zn^{II} ion detection in fibroblast cells with two-photon excitation (TPE) at 710 nm from a Ti:sapphire laser.[12] More recently, owing to their advantageous features such as sharp emission bands, large Stokes shifts, and long excited-state lifetimes in the microsecond range, cell imaging by lanthanide complexes has also received considerable attention. Picot et al. described the two-photon antenna effect of a water-soluble tricationic europium(III) complex with functionalized pyridine carboxylic acid as its ligand [with a two-photon-absorption (TPA) cross section of 19 GM at 760 nm], which was able to label the nucleoli of an ethanol-fixed T24

* To whom correspondence should be addressed. E-mail: bhmhwlam@cityu.edu.hk.
[†] City University of Hong Kong.
[‡] The University of Hong Kong.
[§] Hong Kong Baptist University.
[||] Sun Yat-Sen University.

(1) Denk, W.; Strickler, J. H.; Webb, W. W. *Science* **1990**, *248*, 73–76.
(2) Zipfel, W. R.; Willams, R. M.; Webb, W. W. *Nat. Biotechnol.* **2003**, *21*, 1369−1376, and references cited therein.

10.1021/ic801261h CCC: $40.75
Published on Web 01/07/2009

cancer cell.[13] Law et al. have successfully utilized a terbium(III) complex with a tripodal *N*-[2-(bis{2-[(3-methoxybenzoyl)amino]ethyl}amino)ethyl]-3-methoxybenzamide ligand for three-photon in vitro cell imaging (with a three-photon cross section of 1.9 GM) of different cancer cell types including human lung carcinoma (A549), cervical carcinoma (*HeLa*), and human nasopharyngeal carcinoma (HONE1).[14]

While there are already numerous reports on multiphoton bioimaging using coordination metal and lanthanide complexes as multiphoton luminescent probes, examples of organometallic complexes with two-photon emission properties are scarce and their potentials in bioimaging have not been fully explored.[15] In fact, organometallic complexes are good candidates as multiphoton imaging luminophores. Large TPA cross sections can be brought about by their characteristic intra/interligand and metal-to-ligand charge-transfer transitions during photoexcitation.[16] Spectroscopic and photophysical properties, photostability, water solubility, and the presence of specialized functionalities for organelle- and/or tissue-specific targeting in the organometallic multiphoton probes can be achieved and fine-tuned by the coordination of suitable ligands. Recently, Botchway et al.[17] reported the use of selected cyclometalated platinum(II) complexes for two-photon emission live cell imaging.

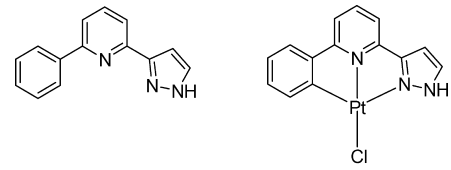

H**L** [Pt(**L**)Cl]

Figure 1. Chemical structures of the C,N,$N_{pyrazolyl}$ cyclometalated ligand H**L** and the corresponding chloro-substituted cyclometalated platinum(II) complex.

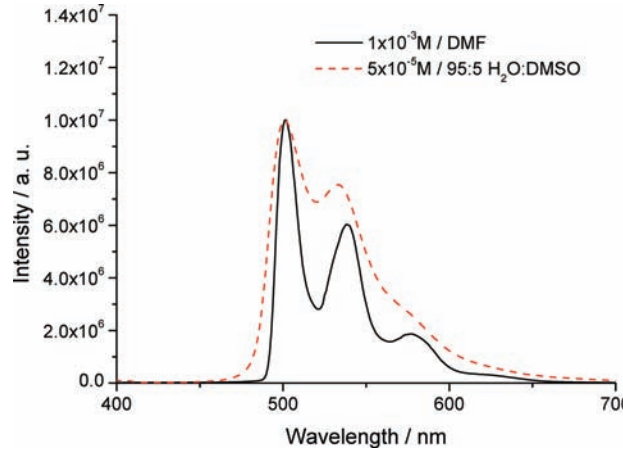

Figure 2. Linear emission spectra of [Pt(**L**)Cl] in DMF (1×10^{-3} M) and in a 95:5 (v/v) aqueous HEPES buffer (pH 7.00)/DMSO (5×10^{-5} M) at 298 K ($\lambda_{ex} = 330$ nm).

We have developed a series of organometallic platinum(II) complexes with a new tridentate cyclometalating ligand 2-phenyl-6-(1*H*-pyrazol-3-yl)pyridine (H**L**), which contains C_{phenyl}, $N_{pyridyl}$, and $N_{pyrazolyl}$ donor moieties (Figure 1).[18] These cyclometalated platinum(II) complexes are photoluminescent in solutions at room temperature. For example, the neutral complex [Pt(**L**)Cl] emits at 500−520 nm in solutions [$\Phi_{lum} = 0.09$, $\tau_0 = 0.57$ μs in *N*,*N*-dimethylformamide (DMF); $\Phi_{lum} = 0.10$, $\tau_0 = 1.46$ μs in 95:5 (v/v) aqueous *N*-(2-hydroxyethyl)piperazine-*N*′-2-ethanesulfonic acid (HEPES) buffer (pH 7.0)/dimethyl sulfoxide (DMSO)]

(3) (a) Bhawalkar, J. D.; Shih, A.; Pan, S. J.; Liou, W. S.; Swiatliewicz, J.; Reinhardt, B. A.; Prasad, P. N.; Cheng, P. C. *Bioimaging* **1996**, *4*, 168–178. (b) Squirrell, J. M.; Wokosin, D. L.; White, J. G.; Bavister, B. D. *Nat. Biotechnol.* **1999**, *17*, 763–767. (c) Pollnau, M.; Gamelin, D. R.; Lüthi, S. R.; Güdel, H. U.; Hehlen, M. P. *Phys. Rev. B* **2000**, *61*, 3337–3346.

(4) (a) Hanson, K. M.; Behne, M. J.; Barry, N. P.; Mauro, T. M.; Gratton, E.; Clegg, R. M. *Biophys. J.* **2002**, *83*, 1682–1690. (b) Douma, K.; Megens, R. T. A.; Reitsma, S.; Prinzen, L.; Slaaf, D. W.; van Zandvoort, M. A. M. J. *Microsc. Res. Tech.* **2007**, *70*, 467–475.

(5) (a) Furuta, T.; Wang, S. S.-H.; Dantzker, J. L.; Dore, T. M.; Bybee, W. J.; Callaway, E. M.; Denk, W.; Tsien, R. Y. *Proc. Natl. Acad. Sci. U.S.A.* **1999**, *96*, 1193–1200. (b) Frederiksen, P. K.; Mclloy, S. P.; Nielsen, C. B.; Nikolajsen, L.; Skovsen, E.; Jørgensen, M.; Mikkelsen, K. V.; Ogilby, P. R. *J. Am. Chem. Soc.* **2005**, *127*, 255–269. (c) Härtner, S.; Kim, H.-C.; Hampp, N. *J. Polym. Sci., Part A* **2007**, *45*, 2443–2452.

(6) (a) Konig, K.; Riemann, I.; Fritzsche, W. *Opt. Lett.* **2001**, *26*, 819–821. (b) Tirlapur, U. K.; Konig, K. *Nature* **2002**, *418*, 290–294.

(7) (a) Albota, M.; Beljonne, D.; Bredas, J.-L.; Ehrlich, J. E.; Fu, J.-Y.; Heikal, A. A.; Hess, S. E.; Kogej, T.; Levin, M. D.; Marder, S. R.; McCord-Maughon, D.; Perry, J. W.; Rockel, H.; Rumi, M.; Subramaniam, C.; Webb, W. W.; Wu, X.-L.; Xu, C. *Science* **1998**, *281*, 1653–1657. (b) Albota, M.; Xu, C.; Webb, X.-L. *Appl. Opt.* **1998**, *37*, 7352–7356. (c) Bestvater, F.; Spiess, E.; Stobrawa, G.; Hacker, M.; Feurer, T.; Porwol, T.; Berchner-Pfannschmidt, U.; Wotzlaw, C.; Acker, H. *J. Microsc.* **2002**, *208*, 108–115. (d) Mongin, O.; Porrès, L.; Moreaux, L.; Mertz, J.; Blanchard-Desce, M. *Org. Lett.* **2002**, *4*, 719–722. (e) Shao, P.; Huang, B.; Chen, L.-Q.; Liu, Z.-J.; Qin, J.-G.; Gong, H.-M.; Ding, S.; Wang, Q.-Q. *J. Mater. Chem.* **2005**, *15*, 4502–4506.

(8) (a) Fu, L.-M.; Wen, X.-F.; Ai, X.-C.; Sun, Y.; Wu, Y.-S.; Zhang, J.-P.; Wang, Y. *Angew. Chem., Int. Ed.* **2005**, *44*, 747–750. (b) Wong, K.-L.; Law, G.-L.; Kwok, W.-M.; Wong, W.-T.; Phillips, D.-L. *Angew. Chem., Int. Ed.* **2005**, *44*, 3436–3439. (c) Picot, A.; Malvolti, F.; Le Guennic, B.; Baldeck, P. L.; Williams, J. A. G.; Andraud, C.; Maury, O. *Inorg. Chem.* **2007**, *46*, 2659–2665.

(9) (a) Auzel, F. *Chem. Rev.* **2004**, *104*, 139–173. (b) Corstiens, P. L. A. M.; Li, S.; Zuiderwijk, M.; Kardos, K.; Abrams, W. R.; Niedbala, R. S.; Tanke, H. J. *IEEE Proc. Nanobiotechnol.* **2005**, *152*, 64. (c) Soukka, T.; Kuningas, K.; Rantanen, T.; Haaslahti, V.; Lovgren, T. *J. Fluoresc.* **2005**, *15*, 513–528.

(10) (a) Larson, D. R.; Zipfel, W. R.; Williams, R. M.; Clark, S. W.; Bruchez, M. P.; Wise, F. W.; Webb, W. W. *Science* **2003**, *300*, 1434–1436. (b) Chakraborty, S. K.; Fitzpatrick, J. A. J.; Phillippi, J. A.; Andreko, S.; Waggoner, A. S.; Bruchez, W. P.; Ballou, B. *Nano Lett.* **2007**, *7*, 2618–2626.

(11) Chang, C. J.; Nolan, E. M.; Jaworski, J.; Okamoto, K.-I.; Hayashi, Y.; Sheng, M.; Lippard, S. J. *Inorg. Chem.* **2004**, *43*, 6774–6779.

(12) Taki, M.; Wolford, J. L.; O'Halloran, T. V. *J. Am. Chem. Soc.* **2004**, *126*, 712–713.

(13) Picot, A.; D'Aléo, A.; Baldeck, P. L.; Grichine, A.; Duperray, A.; Andraud, C.; Maury, O. *J. Am. Chem. Soc.* **2008**, *130*, 1532–1533.

(14) Law, G.-L.; Wong, K.-L.; Man, C. W.-Y.; Wong, W.-T.; Tsao, S.-W.; Lam, M. H.-W.; Lam, P. K.-S. *J. Am. Chem. Soc.* **2008**, *130*, 3714–3715.

(15) (a) Hurst, S. K.; Humphrey, M. G.; Isoshima, T.; Wostyn, K.; Asselberghs, I.; Clays, K.; Persoons, A.; Samoc, M.; Luther-Davices, B. *Organometallics* **2002**, *21*, 2024–2026. (b) Humphrey, J. L.; Kuciauskas, D. *J. Am. Chem. Soc.* **2006**, *128*, 3902–3903. (c) Das, S.; Nag, A.; Goswami, D.; Bharadwaj, P. K. *J. Am. Chem. Soc.* **2006**, *128*, 402–403. (d) Glimsdal, E.; Carlsson, M.; Eliasson, B.; Minaev, B.; Lindgren, M. *J. Phys. Chem. A* **2007**, *111*, 244–250. (e) Zhang, X.-B.; Feng, J.-K.; Ren, A.-M. *J. Phys. Chem. A* **2007**, *111*, 1328–1338.

(16) Zhang, X.-B.; Feng, J.-K.; Ren, A.-M. *J. Organomet. Chem.* **2007**, *692*, 3778–3787.

(17) Botchway, S. W.; Charnley, M.; Haycock, J. W.; Parker, A. W.; Rochester, D. L.; Weinstein, J. A.; Williams, J. A. G. *Proc. Natl. Acad. Sci. U.S.A.* **2008**, *105*, 16071–16076.

(18) Koo, C.-K.; Ho, Y.-M.; Chow, C.-F.; Lam, M. H.-W.; Lau, T. C.; Wong, W.-Y. *Inorg. Chem.* **2007**, *46*, 3603–3612.

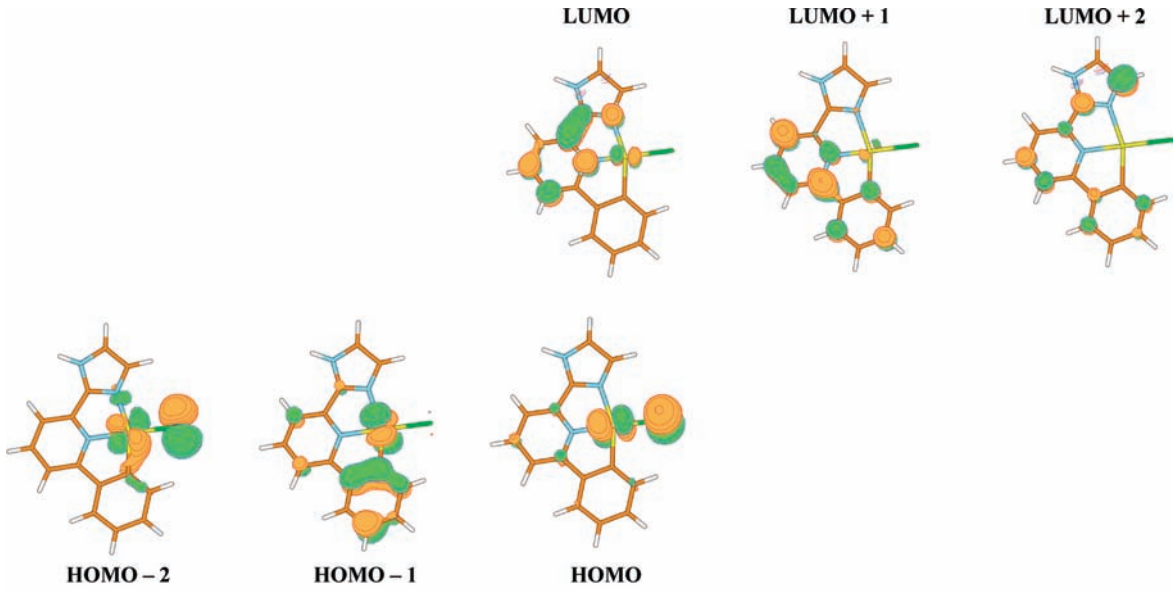

Some frontier molecular orbital energies (ε_i / eV) of [Pt(**L**)Cl]

Orbital	H - 2	H - 1	HOMO[a]	LUMO[b]	L + 1	L + 2
ε_i	-5.8	-5.7	-5.6	-2.5	-2.0	-0.3

[a] HOMO (or H) : the highest occupied molecular orbital; H – 1: the next HOMO.
[b] LUMO (or L) : the lowest unoccupied molecular orbital; L + 1: the next LUMO.

Figure 3. Stereocontour graphs and computed energies of some of the frontier molecular orbitals of [Pt(**L**)Cl] at the level of B3LYP/LANL2DZ.

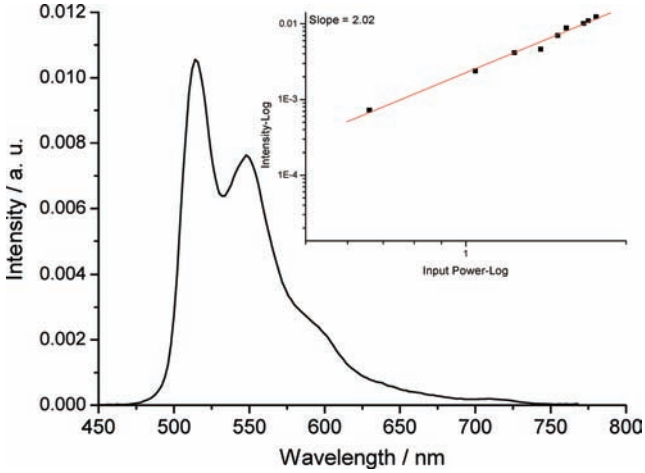

Figure 4. Two-photon-induced luminescent spectra (λ_{ex} = 730 nm) of [Pt(**L**)Cl] in DMF (1×10^{-3} M) at 298 K. The inset shows the power dependence of the emission intensity with a slope of 2.02.

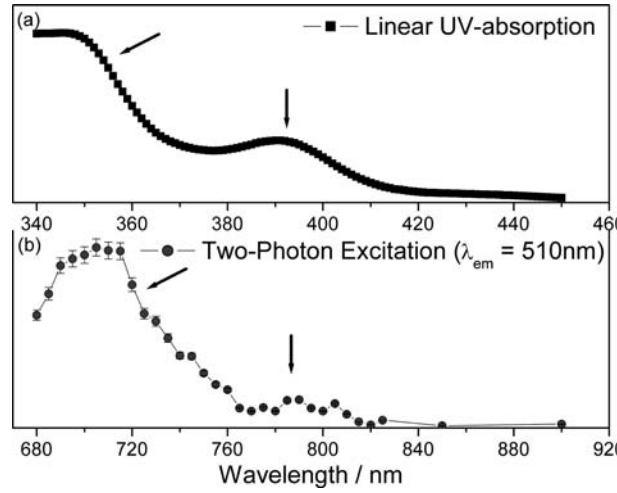

Figure 5. Linear UV−vis absorption (upper) and TPE spectrum (lower) of [Pt(**L**)Cl] in DMF (1×10^{-3} M) at 298 K.

at room temperature when excited at 330 nm (Figure 2). Besides its single-photon photophysical properties, we have recently observed that [Pt(**L**)Cl] can also produce two-photon-induced luminescence. In addition, this complex can be rapidly taken up by live cells within 5 min of exposure and displays relatively low cytotoxicity. Its room temperature multiphoton properties are retained after live cell internalization. All of these suggest that [Pt(**L**)Cl] is a potential multiphoton luminescent probe for in vitro bioimaging.

Experimental Section

Spectroscopic and Photophysical Measurements. UV−vis absorption spectra in the spectral range 200−1100 nm were recorded by a HP UV-8453 spectrophotometer. Single-photon luminescence spectra were recorded using a PerkinElmer LS 50B luminescence spectrophotometer that was equipped with a R928 photomultiplier tube with a 5-nm slit width and 0.5 s integration times at 298 K. The spectra were corrected for detector response and stray background light phosphorescence. Single-photon emission quantum yields were measured by the method of Demas and Crosby[19] and calculated by using the following equation, with $[Ru(bpy)_3](PF_6)_2$ in degassed acetonitrile as the standard (ϕ_r = 0.062):

$$\frac{\varphi_s}{\varphi_r} = \left(\frac{B_r}{B_s}\right)\left(\frac{n_s^2}{n_r^2}\right)\left(\frac{D_s}{D_r}\right)$$

where ϕ is the emission quantum yield, n is the refraction index of the media, D is the integration of the photoluminescent spectrum,

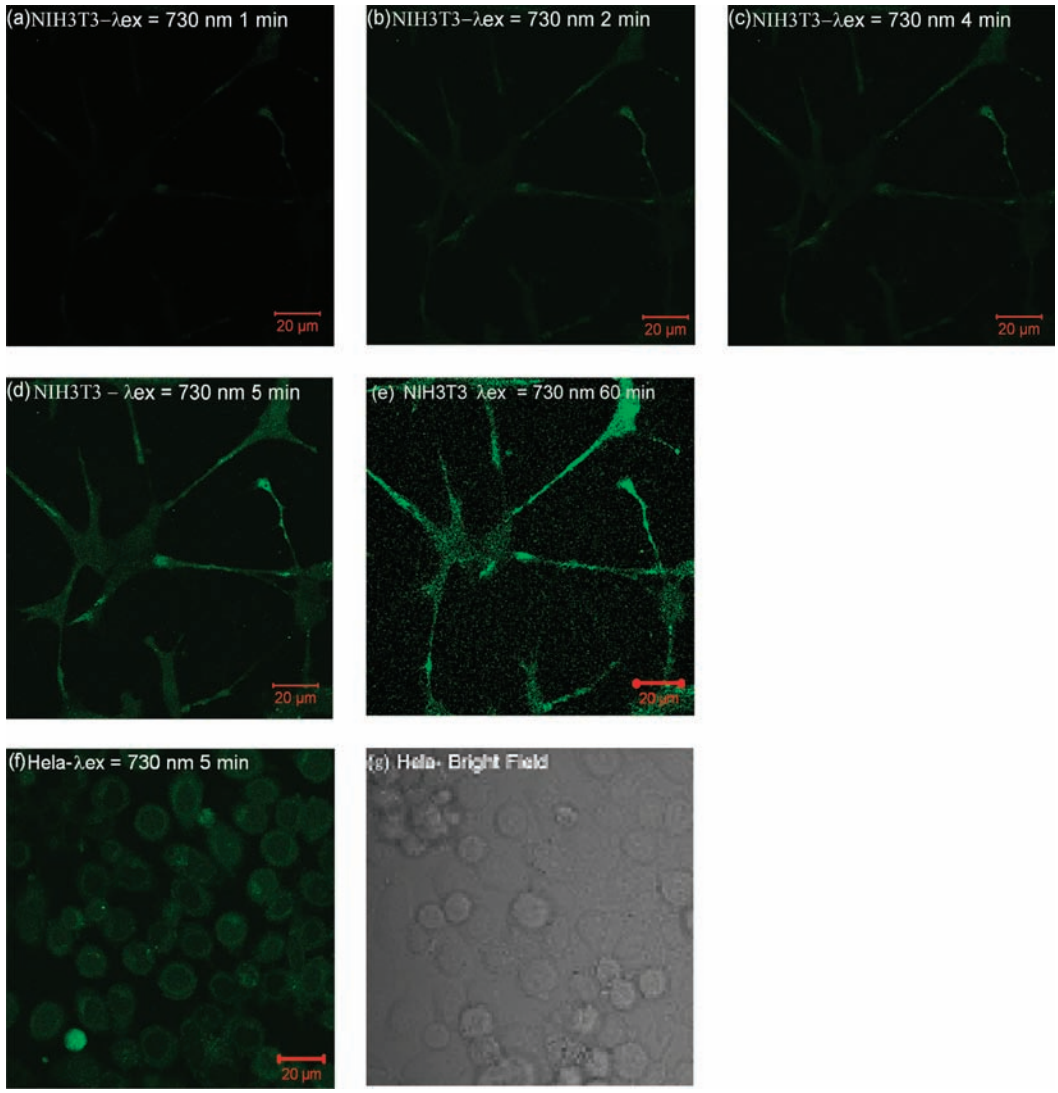

Figure 6. Two-photon confocal microscopy images of NIH3T3 cells after (a) 1, (b) 2, (c) 4, (d) 5, (e) and 60 min of exposure and *HeLa* cells after (f) 5 min of exposure, to [Pt(**L**)Cl] (1 μg/mL in the culture medium, $\lambda_{ex} = 730$ nm, filter band pass for $\lambda_{em} = 500-550$ nm), showing the characteristic green emission at ca. 510 nm of the complex. (g) Bright-field image of the *HeLa* cells of part f (scale bar = 20 μm).

$B = 1 - 10^{-AL}$ (A = absorption and L = light path in solution), and the sample and reference were represented by the subscripts s and r, respectively. Sample and standard solutions were degassed with at least three freeze−pump−thaw cycles. Emission lifetimes were measured by a SPEX Fluorolog 3-TCSPC spectrophotometer in the fast MCS mode with a NanoLED N-370 as the laser source for excitation. The 730-nm pump wavelength was obtained from the fundamental of a femtosecond mode-locked Ti:sapphire laser system (output beam ~ 150 fs duration and 1 kHz repetition rate). The 700−900-nm pump wavelengths were generated from a commercial optical parametric amplifier (Coherent) pumped by the second-harmonic generation of the 800-nm femtosecond pulses. Laser beams were focused to spot size ~50 μm via an $f = 10$ cm lens onto the sample. The emitting light was collected with a backscattering configuration into a 0.5-m spectrograph and detected by a liquid-nitrogen-cooled CCD detector. A power meter was used to monitor the uniform excitation.

Theoretical Calculations. Geometry optimizations were carried out for [Pt(**L**)Cl] in the gas phase using a density functional theory method[20] at the level of B3LYP[21]/LANL2DZ.[22] Stable configurations of the complex were confirmed by the vibrational frequency analysis, in which no imaginary frequency was found for all configurations at the energy minima. All of the computations were performed using the *Gaussian03* program package[23] running on the high-performance computing clusters. In order to clearly understand the related properties of the complex, stereocontour graphs of some of the frontier molecular orbitals in the ground state were drawn with the *Molden* v4.4 program[24] based on the computational results.

Two-Photon-Induced Cross-Sectional Measurements. The theoretical framework and experimental protocol for the two-photon cross-sectional measurement have been outlined by Xu and Webb.[25] In this approach, the TPE ratios of the reference and sample systems are given by

$$\frac{\sigma_2^S \varphi^S}{\sigma_2^R \varphi^R} = \frac{C_R n_S F^S(\lambda)}{C_S n_R F^R(\lambda)}$$

where ϕ is the quantum yield, C is the concentration, n is the refractive index, and $F(\lambda)$ is the integrated photoluminescent spectrum. In our measurements, we ensured that the excitation flux

(19) Demas, J. N.; Crosby, G. A. *J. Phys. Chem.* **1971**, *75*, 991.

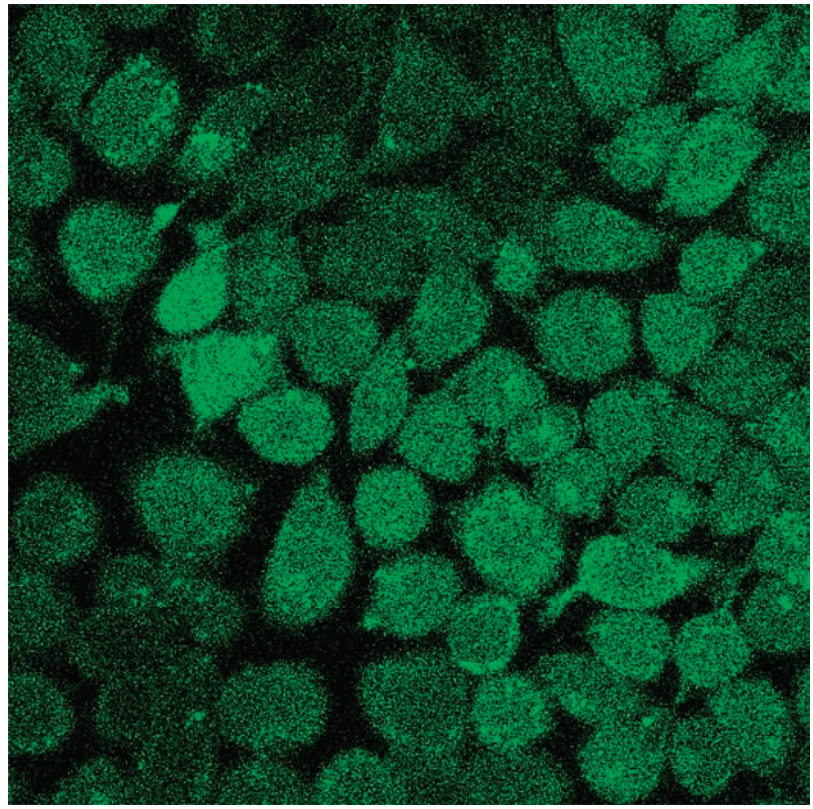

Figure 7. Linear confocal fluorescent microscopy images of *HeLa* cells after 5 min of exposure to [Pt(**L**)Cl] (5 μg/mL in the growth medium, $\lambda_{ex} = 400$ nm, filter band pass for $\lambda_{em} = 500-550$ nm), showing the characteristic emission of [Pt(**L**)Cl] above 500 nm (green).

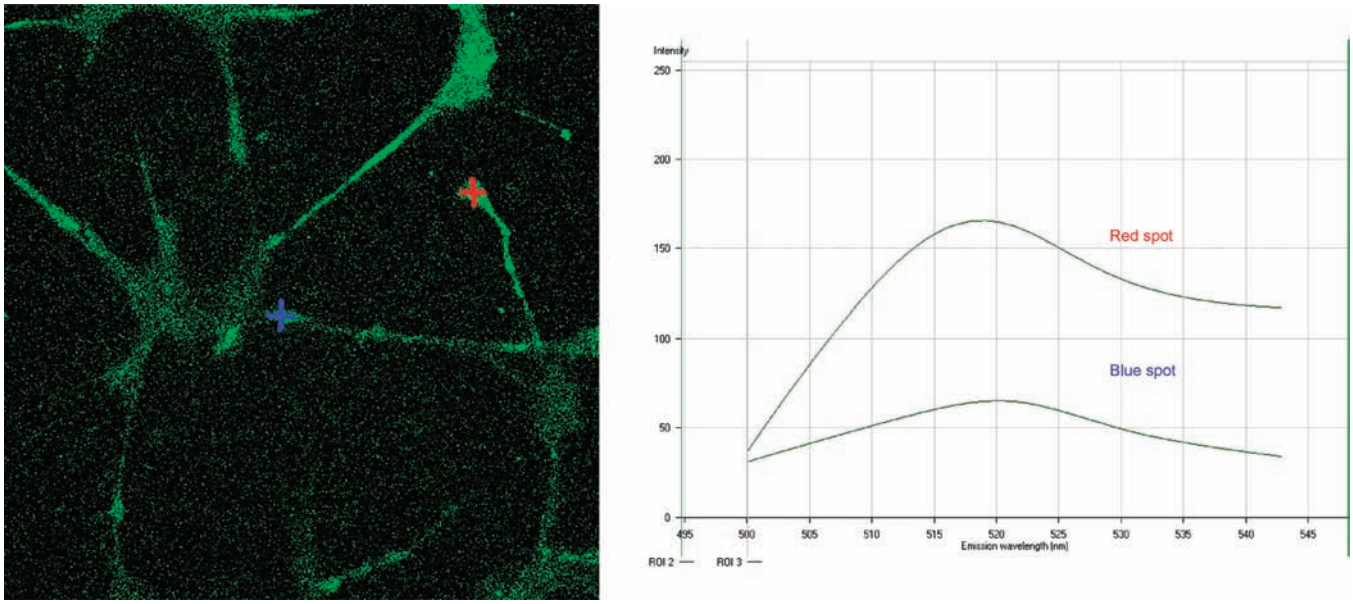

Figure 8. Two-photon confocal fluorescent microscopy images of mouse NIH3T3 cells after 4 h of exposure to [Pt(**L**)Cl] (5 μg/mL in the growth medium, $\lambda_{ex} = 730$ nm, filter band pass for $\lambda_{em} = 500-550$ nm) (left). Emission spectra of the two spots in red and blue obtained by the λ scan of a Zeiss 510 confocal laser fluorescent microscope (right).

and the excitation wavelengths were the same for both the sample and reference. The TPA cross section σ_2 of [Pt(**L**)Cl] was determined using Rhodamine 6G as the reference.[7a]

Microscopy Imaging. For two-photon in vitro imaging, cells were imaged in the tissue culture chamber (5% CO_2, 37 °C) using a Zeiss 510 LSM (upright configuration) confocal microscope equipped with a femtosecond-pulsed Ti:sapphire laser (Libra II, Coherent). The excitation beam produced by the femtosecond laser, which was tunable from 720 to 900 nm ($\lambda_{ex} = 730$ nm, ~1.5 mW), passed through an LSM 510 microscope with HFT 650 dichroic (Carl Zeiss, Inc.) and focused on coverslip-adherent cells using a 63× oil immersion objective. The NLO META scan head allowed data collection in 10.7 nm windows at 510 nm, and a bypass filter of 500−550 nm was used for collection of the emission light.

(20) (a) Becke, A. D. *J. Chem. Phys.* **1993**, *98*, 1372–1377. (b) Görling, A. *Phys. Rev. A* **1996**, *54*, 3912–3915. (c) Foresman, J. B.; Frisch, Æ. *Exploring Chemistry with Electronic Structure Methods*, 2nd ed.; Gaussian Inc.: Pittsburgh, PA, 1996.

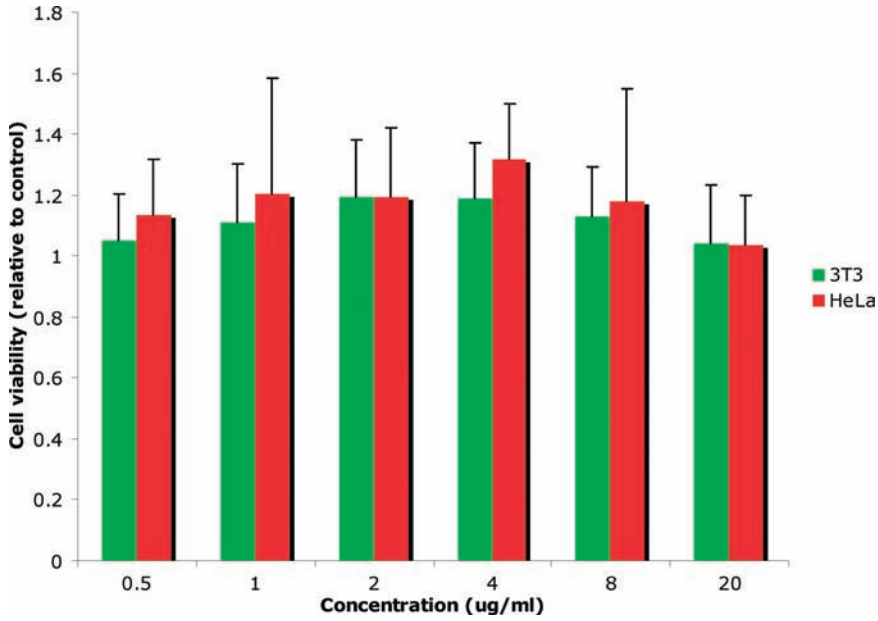

Figure 9. MTT assays of cytotoxicity of [Pt(**L**)Cl] on mouse NIH3T3 and *HeLa* cells.

Cell Culture. Human cervical carcinoma (*HeLa*) cells and mouse skin fibroblasts (NIH3T3; nos. CCL-2 and 72-13G; American type Culture Collection, Manassas, VA) were maintained in an RMPI 1640 medium (*HeLa*) and DMEM medium (NIH3T3) supplemented with 10% fetal bovine serum and 1% penicillin and streptomycin in 5% CO_2. For the imaging, 0.5×10^6 cells were seeded onto 60 $\times$ 15 mm culture dishes at 2 mL/dish (MatTek Corp., Ashland, MA), as previously. The cells were allowed to attach overnight. The cell medium in each well was changed immediately prior to the initiation of the exposures.

MTT Assay. The cell growth rate was measured using a 3-(4,5-dimethylthiazol-2-yl)-2,5-diphenyltetrazolium bromide (MTT) proliferation assay kit according to the manufacturer's instructions (Roche Diagnostics). Briefly, 3000 cells were seeded in 96-well plates and cultured in 5% fetal calf serum for 24 h. Taxol was added 24 h after plating, and the cell viability was examined at 24 h postexposure. Before testing, 10 μm of MTT labeling reagent (5 mg/mL MTT in PBS) was added, and the cells were incubated for a further 4 h at 37 °C. Then, 100 μL of solubilizing reagent (10% sodium dodecyl sulfate in 0.01 mol/L HCl) was added, and the plate was incubated overnight at 37 °C to dissolve the formazan crystals. The absorbance was measured at a wavelength of 570 nm on a Labsystem Multiskan microplate reader (Merck Eurolab, Dietikon, Switzerland). Each time point was conducted in triplicate wells, and each experiment was repeated twice. Each data point represented the mean and standard derivation.

Results and Discussion

Synthesis and Linear Photophysical Properties. The synthesis and linear photophysical properties for [Pt(**L**)Cl] have been previously reported, with its molecular structure characterized by X-ray crystallography.[18] In short, [Pt(**L**)Cl] possesses intense absorption bands at 275−375 nm and moderately intense absorption bands at 380−410 nm, which were assigned intraligand (IL) and singlet metal-to-ligand charge-transfer (^{1}MLCT) [dπ(Pt) $\rightarrow$ π^*(**L**)] transitions, respectively. Figure 3 shows the stereocontour graphs and computed energies of some of the frontier molecular orbitals of [Pt(**L**)Cl] obtained at the level of B3LYP/LANL2DZ. The highest occupied molecular orbital (HOMO) has electron density distributed on the platinum metal center and the chloride ligand, while the lowest unoccupied molecular orbital (LUMO) has electron density mainly distributed on the tridentate cyclometalating ligand **L**. The energy difference of ca. 3.1 eV between the HOMO and LUMO corresponded to the absorption at ca. 400 nm of the complex for the transition to its ^{1}MLCT excited state. Upon linear photoexcitation at 330 nm, [Pt(**L**)Cl] exhibits intense green emission under ambient conditions, with a structured emission profile centered at ca. 510 nm. The origin of the emission was previously assigned the ^{3}MLCT [dπ(Pt) $\rightarrow$ π^*(L)] excited state in accordance with the literature spectroscopic characterizations of the analogous cycloplatinated system [Pt(C$\wedge$N$\wedge$N)Cl] (where HC$\wedge$N$\wedge$N = 6-phenyl-2,2′-bipyridine).[18,26]

Two-Photon-Induced Photophysical Studies. Figure 4 shows the emission spectrum of [Pt(**L**)Cl] in DMF (1×10^{-3}

(21) Lee, C.; Yang, W.; Parr, R. G. *Phys. Rev. B* **1988**, *37*, 785–789.
(22) (a) Hay, P. J.; Wadt, W. R. *J. Chem. Phys.* **1985**, *82*, 270. (b) Wadt, W. R.; Hay, P. J. *J. Chem. Phys.* **1985**, *82*, 284. (c) Hay, P. J.; Wadt, W. R. *J. Chem. Phys.* **1985**, *82*, 299.
(23) Frisch, M. J.; Trucks, G. W.; Schlegel, H. B.; Scuseria, G. E.; Robb, M. A.; Cheeseman, J. R.; Montgomery, J. A.; Vreven, T., Jr.; Kudin, K. N.; Burant, J. C.; Millam, J. M.; Iyengar, S. S.; Tomasi, J.; Barone, V.; Mennucci, B.; Cossi, M.; Scalmari, G.; Rega, N.; Petersson, G. A.; Nakatsuji, H.; Hada, M.; Ehara, M.; Toyota, K.; Fukuda, R.; Hasegawa, J.; Ishida, M.; Nakajima, T.; Honda, Y.; Kitao, O.; Nakai, H.; Klene, M.; Li, X.; Knox, J. E.; Hratchian, H. P.; Cross, J. B.; Bakken, V.; Adamo, C.; Jaramillo, J.; Gomperts, R.; Stratmann, R. E.; Yazyev, O.; Austin, A. J.; Cammi, R.; Pomelli, C.; Ochterski, J. W.; Ayala, P. Y.; Morokuma, K.; Voth, G. A.; Salvador, P.; Dannenberg, J. J.; Zakrzewski, V. G.; Dapprich, S.; Daniels, A. D.; Strain, M. C.; Farkas, O.; Malick, D. K.; Rabuck, A. D.; Raghavachari, K.; Foresman, J. B.; Ortiz, J. V.; Cui, Q.; Baboul, A. G.; Clifford, S.; Cioslowski, J.; Stefanov, B. B.; Liu, G.; Liashenko, A.; Piskorz, P.; Komaromi, I.; Martin, R. L.; Fox, D. J.; Keith, T.; Al-Laham, M. A.; Peng, C. Y.; Nanayakkara, A.; Challacombe, M.; Gill, P. M. W.; Johnson, B.; Chen, W.; Wong, M. W.; Gonzalez, C.; Pople, J. *Gaussian03*, revision D.1.A; Gaussian, Inc.: Wallingford, CT, 2005.
(24) Schaftenaar, G.; Noordik, J. H. *J. Comput.-Aided Mol. Des.* **2000**, *14*, 123–134.
(25) Xu, C.; Webb, W. W. *J. Opt. Soc. Am. B* **1996**, *13*, 481–491.

M) after excitation at 730 nm by a femtosecond mode-locked Ti:sapphire laser. The spectrum corresponds well with that obtained by single-photon excitation (Figure 2). The TPA process was confirmed by a power dependence experiment (inset of Figure 4) and the two-photon near-infrared excitation spectra (Figure 5). It is worth noting that the nonlinear excitation spectrum of [Pt(**L**)Cl] possesses the same band shape compared to its UV−vis absorption spectrum except that the corresponding wavelength is doubled. This implies that TPA is capable of populating both the $\pi \rightarrow \pi^*$ IL and MLCT transition states. Similar phenomena of the population of the IL and MLCT excited states of ruthenium(II) complexes with fluorine-substituted 1,10-phenanthroline ligands by TPA have also been recently reported by Lemercier and Andraud.[27] The TPA cross section of [Pt(**L**)Cl] was measured with Rhodamine 6G[7a,28] in DMF to be 20.8 GM, which is much higher than the value suggested by Furuta et al.[5a] for biological applications in live specimens (0.1 GM). This cross section is also greater than those of the recently reported cycloplatinated complexes by Botchway et al. (∼4 GM)[17] as well as the previous reported platinum(II) acetylide complexes by Glimsdal et al. (5−10 GM).[15d]

In Vitro Cell Imaging. *HeLa* and NIH3T3 cells were exposed to [Pt(**L**)Cl] at a concentration of 1 μg/mL for various time durations (0−60 min). Upon 1−2 min of exposure, green luminescence was observable in the NIH3T3 cells, which was revealed as punctuated patterns under 400- and 730-nm femtosecond laser excitations (Figure 6a,b). After a further 1 min of exposure, more cells were found to exhibit stronger green luminescence (Figure 6c). At an exposure time of up to 5 min, more than 95% of the cells exhibited green luminescence (Figure 6d). A similar fluorescent imaging phenomenon was observed in *HeLa* cells with both linear and TPEs as shown in Figures 6f and 7. The bright-field morphology of these examined cells is shown in Figure 6g. Interestingly, all of the intracellular luminescence images were readily observable without the need of prior washing to remove [Pt(**L**)Cl] in the medium. In fact, the complex was rapidly taken up and accumulated in the cells. This behavior is very different from many of the commercially available fluorescent dyes, which function solely by diffusion along a concentration gradient. In those cases, live cell imaging has to be proceeded using a relatively high concentration of dyes, which might have adverse effects on the cell metabolism and physiology. The presence of a high concentration of dye in the culture medium also necessitates its removal, via extensive washing, before imaging can be carried out. With a bioaccumulative dye, a much lower loading of dye and a much shorter incubation time are sufficient for cell staining. Moreover, the emission of the washing step allows the internalization process of the dye into living cells to be visualized by time-lapsed microscopy.

Emission spectra of [Pt(**L**)Cl] inside *HeLa* and NIH3T3 cells were recorded by the λ scan system of a Zeiss 510 confocal laser fluorescent microscope (Figure 8). These emission spectra exhibited similar bands centered at 500−520 nm, which were comparable to that of [Pt(**L**)Cl] in solution (Figure 2). The apparent loss of the luminescent fine structures may be attributable to the difference in the properties of the media within live cells from the aqueous−organic solvent systems adopted in spectroscopic and photophysical measurements. Nevertheless, this observation suggests that the nature of the emission from the cyclometalated platinum complex before and after entering the cells is the same.

Cytotoxicity Study. Cytotoxicity of [Pt(**L**)Cl] to the tested cell lines was low. MTT assays on *HeLa* and NIH3T3 cells exposed to as high as 20 times the dose concentration of the organometallic complex for imaging for 6 h showed viability similar to that of the controls (Figure 9). This low cytotoxicity of [Pt(**L**)Cl] is consistent with that observed by Botchway et al.[17] in their series of cyclometalated platinum(II) complexes on a CHO K1 animal-derived cell line. Binding to biomolecules in the intracellular hydrophobic environment has probably reduced the production of singlet oxygen from the quenching of excited [Pt(**L**)Cl]* species by dioxygen.

Conclusions

In summary, the organometallic cyclometalated platinum(II) complex [Pt(**L**)Cl] is found to exhibit strong two-photon-induced emission with a relatively high cross section and good live cell internalization properties. The multiphoton luminescence, fast bioaccumulation in live cells, and relatively low cytotoxicity of [Pt(**L**)Cl] render it a useful multiphoton bioimaging probe. Like other coordination and organometallic complexes, the properties of this cyclometalated platinum(II) system can be further fine-tuned by modification of both the ancillary and cyclometalating ligands. Works on evaluating the bioimaging properties of this class of cycloplatinated complexes are in progress.

Acknowledgment. The authors acknowledge financial support from the Hong Kong Research Grants Council, City University of Hong Kong, and Hong Kong Baptist University. K.-L.W. acknowledges a Research Scholarship Enhancement Scheme from City University of Hong Kong.

IC801261H

(26) (a) Lu, W.; Chan, M. C.-W.; Cheung, K.-K.; Che, C.-M. *Organometallics* **2001**, *20*, 2477–2486. (b) Hofmann, A.; Dahlenburg, L.; Eldik, R. *Inorg. Chem.* **2003**, *42*, 6528–6538. (c) Kui, S. C. F.; Chui, S. S.-Y.; Che, C.-M.; Zhu, N. *J. Am. Chem. Soc.* **2006**, *128*, 8297–8309.

(27) (a) Girardot, C.; Lemercier, G.; Mulatier, J.-C.; Chauvin, J.; Baldeck, P. L.; Andraud, C. *Dalton Trans.* **2007**, 3421–342. (b) Girardot, C.; Cao, B.; Mulatier, J.-C.; Baldeck, P. L.; Chauvin, J.; Riehl, D.; Delaire, J. A.; Andraud, C.; Lemercier, G. *ChemPhysChem* **2008**, *9*, 1531–1535.

(28) Kohl, T.; Heinze, K. G.; Kuhlemann, R.; Koltermann, A.; Schwille, P. *Proc. Natl. Acad. Sci. U.S.A.* **2002**, *99*, 12161.